

C₂H₃ oxidation/dehydrogenation competition in Methane Mild Combustion

¹M. de Joannon, ²P. Sabia, ¹A. Tregrossi, ³T. Faravelli, ³E. Ranzi, ²A. Cavaliere

1. Istituto di Ricerche sulla Combustione - C.N.R., Naples

2. Dip. di Ingegneria Chimica - Università Federico II, Naples

*3. Dip. di Chimica, Materiali ed Ingegneria Chimica– Politecnico di Milano
ITALY*

INTRODUCTION

Mild Combustion conditions (i.e. highly pre-heated and very diluted reactants) have been shown to influence the fuel oxidation kinetic significantly [1, 2]. The very high initial temperature and the very low concentration of reactants strongly modify the competitions among the different kinetic pathways thus stressing behavior that are usually hidden in traditional combustion conditions by very fast oxidation process both for high and low molecular weight hydrocarbons. Therefore, a large scale application of Mild Combustion requires the systematic evaluation of the effects of high inlet temperatures and high dilution degrees on fuel oxidation.

For low molecular weight hydrocarbons, a preliminary study was carried out [3] which investigated methane oxidation under Mild conditions by means of experimental and numerical analyses performed on a continuous stirred flow reactor.

The extreme working conditions revealed significant temperature oscillation phenomenology for a relatively wide range of inlet temperatures and C/O ratios that was classified on the basis of waveform shape. The only experimental evidence reported in the literature in relation to oscillatory behaviors in methane oxidation was obtained at lower temperatures and under batch conditions [4]. From a practical point of view, the presence of such oscillatory regimes could give rise to high frequency oscillations in combustion chambers, which are generally responsible for decreasing the efficiency of and causing serious damage to gas turbine burners.

In this paper, the main process parameters affecting all types of combustor are analyzed in detail by means of a direct comparison between the experimental measurements made in a Jet Stirred Reactor and numerical predictions based on a chemical kinetic scheme developed for general use.

EXPERIMENTAL SET-UP

The measurements were carried out on experimental configurations used extensively for the study of C₅-C₇ low temperature oxidation [5] and shown in Figure 1a. A spherical quartz Jet Stirred Flow Reactor (volume=0.1dm³) was placed inside a cylindrical electrically-heated, ceramic fiber wall oven. The oxygen/nitrogen mixture and methane were pre-heated separately to the oven temperature and then fed into the pre-mixing section of the reactor where the fluid-dynamic conditions inhibit the occurrence of any chemical reaction. The mixture was then introduced into the reactor by means of four jet nozzles sketched in figure 1a. Each jet was oriented differently so that the direction and velocity of the gas flow at the jet outlets would ensure well-mixed conditions across a relatively wide range of residence

times. Therefore, using methane as tracer in a nitrogen flow, the obtained Residence Time Distribution (RTD) function E was analyzed by means of the “Tanks-in-series” model. The results suggested the jet reactor behaves such as a well mixed reactor for residence time lower than 0.6 sec.

However, in order to continuously monitor the reactor behavior in oscillation regimes a two-dimensional visualization system was set up. An intensified CCD camera, sensible in a wide spectral range, from 200 nm up to 700 nm, was used in order to collect the spontaneous light emitted from the reacting volume.

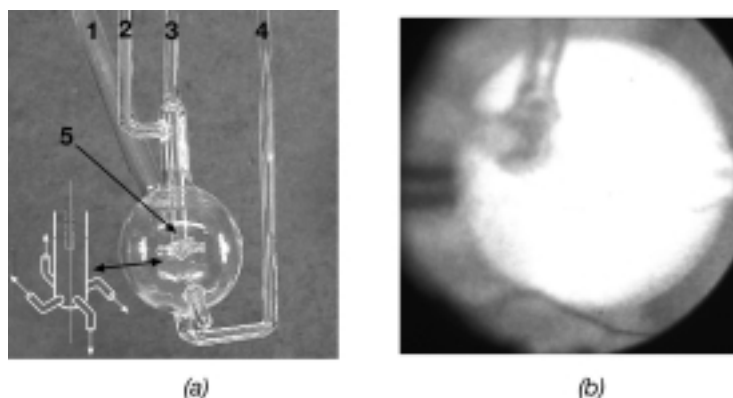


Figure 1: (a) Jet Stirred Flow Reactor used in the experimental analysis: 1) Thermocouple duct; 2) Oxygen/nitrogen inlet; 3) Fuel inlet; 4) Exhaust outlet; 5) Reactant premixing section.

(b) Reactor image detected by the CCD camera for $T_{inlet} = 1125$ K and a C/O = 0.3 during oscillations

In Figure 1b the reactor image, detected during oscillations for an inlet temperature of 1125 K and a C/O ratio equal to 0.3 (C/O=fuel C atoms/oxidant O atoms), shows that the luminous signal can be detected from the whole reactor volume and it is uniformly distributed. The same results were obtained in the most of the experimental conditions here considered thus testifying that the system works in well-mixed conditions.

Experimental tests were carried out at atmospheric pressure. The dilution level was fixed by setting the nitrogen volumetric fraction at 90% and C/O was increased from 0.01 to 1.4. For each C/O, the inlet reactant temperature (T_{inlet}) was changed from 825K to 1275K. The residence time, τ , was set to 0.5sec that ensures well mixed working conditions.

Time-resolved profiles of the reactor temperature were measured using a silica coated fine wire (40 μ m bead size) Pt-Pt13%Rh thermocouple.

Sampling and off-line analyses by means a gas chromatograph equipped with Poraplot Q column and a flame ionization detector for the determination of C₂ saturated and unsaturated hydrocarbons were carried out in selected conditions.

In this work two different kinetic mechanisms were used in order to simulate the methane combustion process in Mild condition. The mechanism implemented by Ranzi et al. (TOT0310) [6, 7, 8] consisting of 250 species involved in more than 5000 reactions, and the one implemented by Warnatz et al. [9] that considers 34 species and 164 reactions have been used for the numerical analysis of methane oxidation.

Two different software were used in order to simulate experimental results. In fact Ranzi et al. [10] developed also a specific code (DSMOKE) to simulate a variety of flame and combustion processes. On the other hand the “Warnatz” mechanism was in such a format to be readable and compiled by ChemKin 3.6 software [11]. Both of these codes can simulate the behavior of perfect stirred reactor (PSR) reactors in transient and not adiabatic conditions. Respectively the former code uses the PSR application and the latter the AURORA

application [12] in not-steady conditions.

RESULTS AND DISCUSSION

Behavior of the $\text{CH}_4/\text{O}_2/\text{N}_2$ mixture in Mild conditions for different dilution levels has been discussed in previous papers [3, 13]. It was shown that in correspondence of experimental settings considered, unreactive, steady combustion and dynamic working conditions are reached in dependence on inlet temperature and C/O ratio values. Moreover, a comparison between experimental and numerical results demonstrated that the dynamical behavior encountered during methane oxidation is due to the interaction between the oxidation/recombination kinetics of methane and the thermal exchange between the reactor and the environment [3, 13]. It was pointed out that C_2 reaction kinetic plays a not secondary role in this phenomenology. Once the ethane is formed, it is mainly dehydrogenated until the formation of vinyl radicals (C_2H_3). They can either oxidize with the formation of oxygenated species or can dehydrogenize, yielding C_2H_2 .

In order to point out the relative weight of different kinetic pathway in recombination mechanism, a comparative analysis of reactor temperature (T_R) and C_2 concentrations measured for different experimental conditions has been carried out.

In Figure 2 T_R are reported as a function of T_{inlet} on T_{inlet} for C/O of 0.5 and 0.1. Solid lines in the diagrams represent conditions where the system reaches a steady working temperature whereas the dotted lines represent the maximum (T_{max}) and minimum (T_{min}) temperatures measured during the oscillations. Moreover, the dashed line is used to extrapolate a possible unstable steady state in the region of hysteresis, which would not be detectable by means of any experimental analysis. On the coordinate axis, shown on the right-hand side of the same diagram, the C_2H_6 and $\text{C}_2\text{H}_4\text{-C}_2\text{H}_2$ concentrations measured in the same experimental conditions of temperature profiles are also reported. The temperature profile measured for C/O=0.5 shows the typical “S” shape found in the presence of a steady state multiplicity. The lower branch of the temperature profile in the hysteresis region lies on the isothermal line up to $T_{\text{inlet}}=925\text{K}$. For $T_{\text{inlet}}=975\text{K}$, a temperature increase of about 20K was recorded. In the same region, the upper branch of the hysteresis is characterized by a T_R varying from 1129K to 1285K. ΔT is nearly constant up to $T_{\text{inlet}} = 1150\text{K}$.

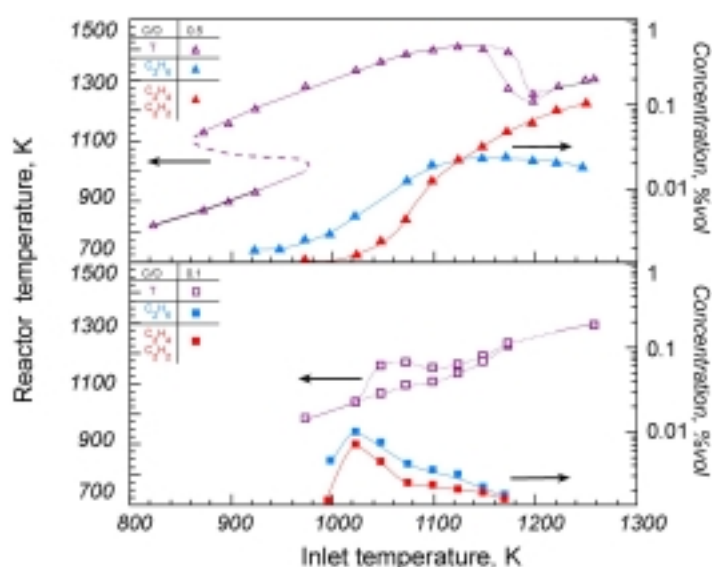


Fig. 2: Reactor temperature and $\text{C}_2\text{H}_6/\text{C}_2\text{H}_4\text{-C}_2\text{H}_2$ concentration profiles versus T_{inlet} at C/O=0.5 (a) and C/O=0.1 (b).

In this temperature range, C_2H_6 and $C_2H_4-C_2H_2$ concentrations increase with T_{inlet} . At $T_{inlet}=1150K$, T_R reaches its maximum value, then drops towards the isothermal line and, for temperatures higher than 1225 K, it comes very close to T_{inlet} . In correspondence with the maximum temperature, the $C_2H_4-C_2H_2$ concentration becomes equal to C_2H_6 . Interestingly, this occurs before the onset of oscillation. After that, C_2H_6 reaches a maximum and then becomes nearly constant whereas $C_2H_4-C_2H_2$ increases continuously up to 1275K.

Different considerations apply to $C/O=0.1$ (fig.2b). In this case both C_2H_6 and $C_2H_4-C_2H_2$ grow with temperature up to $T_{inlet}=1000K$ where they reach a maximum. At $T_{inlet}=1125K$, the temperature oscillations start and both C_2H_6 and $C_2H_4-C_2H_2$ decrease.

A comparison among the experimental and the numerical $T_{inlet}-C/O$ maps of system behavior at 90% of dilution level is reported in Figure 3. Both the two numerical models used in this work are able to reproduce the system dynamic behavior. In particular they simulate also the most of the different typologies of oscillations that have been found experimentally. In particular, the TOT0310 mechanism simulates oscillations between 1030K and 1275K for $C/O=0.05-0.1$. By increasing the C/O , the dynamic region shrinks, covering a shorter temperature range, and disappears when the C/O is higher than 0.45. Up to this C/O value, the left-hand boundary of the region follows that of the experimental dynamic area quite well. In contrast, the right edge limits the oscillation region to a temperature range which is smaller than the one corresponding to the experimental area.

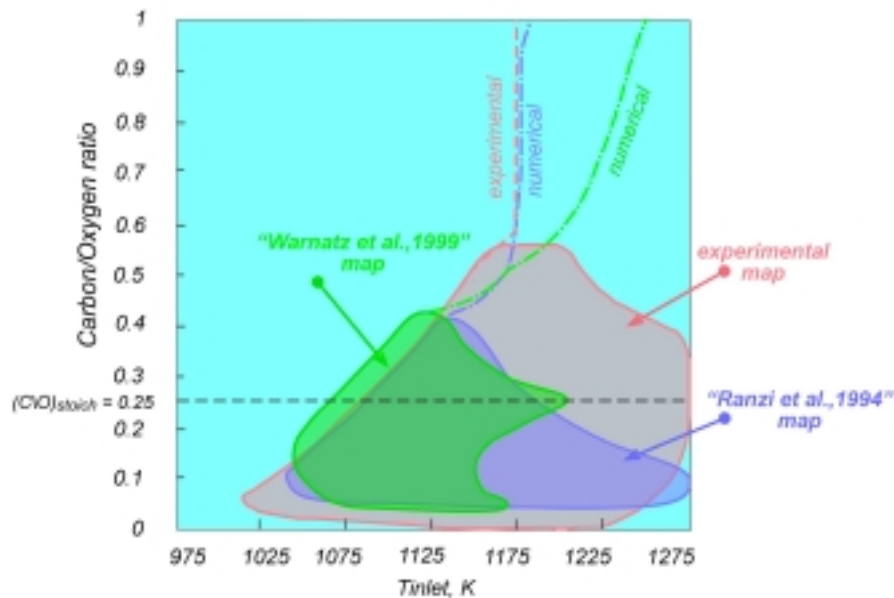


Fig3 Comparison among experimental and numerical maps at 90% of dilution level.

Even though also the “Warnatz” model is able to simulate temporal oscillations, the extension of the dynamic region identified with such a model is less wide. In particular, for C/O ratio values comprised between 0.05 and 0.1 the oscillation have been detected between 1050K and 1175K. Also in this case, increasing C/O oscillations are detected for a smaller temperature range and then disappear for $C/O = 0.4$. Only for stoichiometric C/O value ($C/O_{stoich.}=0.25$) the region enlarges up to 1215 K. For $C/O > 0.25$ the right side of the two numerical regions almost coincide.

The same numerical analysis was performed using the “Warnatz” model in a previous work [3] and the shape of the area in which oscillations have been numerically detected is similar but the area covers a wider temperature range. This is due to the different heat transfer

coefficient used for simulations in this paper. In fact, at the light of thorough calculations and experimental evaluation, the heat transfer coefficient has been assessed to be equal to one half of the value used in other works. The use of a different coefficient underlines the dependence of the dynamic region on this parameter and in particular it comes out that the smaller it is, the smaller the extension of the area where oscillations occur is.

In the stable combustion region, the dashed-dotted curves in figure 3 represents the numerically computed loci of maximum temperature increase for a fixed C/O. The “Ranzi et al.” model quite ably reproduces the curve obtained by means of the experimental analysis (dashed line). On the contrary the “Warnatz” model line does not fit experimental values.

The TOT0310 kinetic mechanism seems to work better than the “Warnatz” mechanism for high temperatures in fact it reproduces better the extension of dynamic region for C/O ratios lower than the stoichiometric value and it fits quite well the experimental line that identifies inlet conditions for which the maximum temperature increase is detectable.

The TOT0310 mechanism was used to perform a preliminary study on the identification of the main kinetic pathways of the recombination channel. In order to evaluate the relative weight of oxidation and dehydrogenation channels of C_2 species, the rates of the reactions responsible for C_2H_3 consumption were evaluated as function of T_{inlet} . The results at $C/O = 0.5$ were reported in Figure 4a where the dashed red curve represents the rate of C_2H_3 oxidation whereas the solid blue line indicates the rate of C_2H_3 dehydrogenation to C_2H_2 . The rate of C_2H_3 oxidation increases up to $T_{inlet}=1175K$. As shown by dashed-dotted line in Figure 2, this temperature corresponds to the highest ΔT computed at $C/O=0.5$. In the same temperature region, the rate of C_2H_3 dehydrogenation increases continuously with T_{inlet} even though it always remains lower than C_2H_3 oxidation rate. From $T_{inlet}=1175K$ onwards, the rate of C_2H_3 oxidation decreases and is overwhelmed at about $T_{inlet}=1275K$ by C_2H_3 dehydrogenation which continues to rise.

The same analysis was performed for $C/O=0.1$, i.e. under lean conditions. Results are showed in figure 4b. From $T_{inlet}=1000 K$ up to $T_{inlet}=1050 K$, C_2H_3 oxidation is the only active channel of C_2H_3 consumption. It reaches an initial maximum at $T_{inlet}=1025K$ then decreases up to $T_{inlet}=1050K$. Higher T_{inlet} corresponds to a temperature oscillation region, where the reaction rates represent the mean value computed for a single oscillation period. With the onset of oscillation, both oxidation and dehydrogenation reactions increase. The former reach a maximum at 1150K, then decrease but still remain higher than the C_2H_3 dehydrogenation rate. At $T_{inlet}=1050K$, the C_2H_3 dehydrogenation rate suddenly reaches a nearly constant value and remains that way until 1300K before falling steeply to very low values.

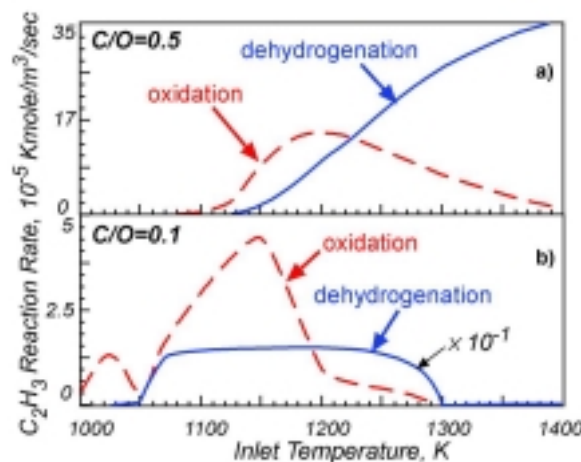


Fig. 4 C_2H_3 reaction rate for oxidation and dehydrogenation channel at $C/O=0.5$ and $C/O=0.1$

The plots versus T_{inlet} show that the C_2H_6 concentration is higher than the C_2H_4 and C_2H_2 concentrations in a temperature range where there is a significant increase in reactor temperature. In other words, the recombination channel is active in these regions and the pyrolytic products, such as acetylene, are not the prevalent final products. In fact, for temperatures higher than 1100K-1200K, acetylene is prevalent and endothermic reactions are favored with respect to oxidative ones. The same trends were measured for higher C/O, but these are not reported here.

A clear insight can be drawn from the kinetic scheme analysis in the region where the comparison between experimental and numerical results is very satisfactory. This is around the loci of the measured and predicted maximum temperature increase, as is reported in the Figure 3. In fact they almost coincide for C/O higher than 0.5 since they are both situated on a line at a nearly constant temperature around 1180K. It is noteworthy that the predicted maximum production rate for C_2H_3 oxidation is placed around this temperature for C/O=0.5, as it is shown in Figure 4a. In the same temperature region, a steep increase in acetylene production from the same C_2H_3 radical is predicted. To summarize, Figure 4 shows that the dehydrogenation and oxidation of vinyl radicals are in competition and a temperature around 1200K marks the separation point between the two ranges in which one of the two is dominant.

The same analysis of the vinyl radical destruction channels has been performed at C/O=0.1. Figure 4b depicts the plot pertaining to this comparison. The rate of oxidation is higher than the dehydrogenation of the vinyl radical in a temperature region where oscillations occur. When this channel disappears, the oscillations also disappear.

CONCLUSION

First of all both the two mechanisms are able to reproduce the dynamic behavior detected experimentally. In particular the “Ranzi et al.” kinetic model seems to simulate better than the “Warnatz” mechanism the extension of the region where oscillation occurs maybe for the richness of species and reactions that form the mechanism itself. Anyway this experimental evidences represent a rigorous test for validation of kinetic models that must be able to predict the dynamic behavior of the reacting system, thus considering more stringent constraints.

Furthermore if these experimental results are analyzed from a practical point of view it is possible to recognize two main features.

The first is that diluted combustion processes cannot be performed without an accurate analysis of the auto-ignition process. This fact is broadly acknowledged for large paraffins [14, 15], but it has been completely ignored with regard to low mass molecular species, such as methane.

In this case, relatively high air temperatures in excess of 1400K must be obtained to achieve stable conditions for all air/fuel ratios, whereas temperatures above 1000K are high enough if the mixture is twice as rich as the stoichiometric C/O. This is consistent with the noiseless operation of many Flameless Combustion processes reported in the literature [2, 16]. In fact, these types of combustors are designed in such a way that fuel is injected into the high temperature recirculation flow with oxygen starvation and only a second stage of mixing with air ensures the further completion of the oxidation. In this case, the oxidation region was experimentally identified. This had been predicted in a previous paper by means of a steady numerical model [17], in which the recombination of smaller radicals into $C_{(2)}$ species was minimized.

A second feature pertains to the identification of the kinetic mechanism, which is responsible for exothermicity-damping at relatively high temperatures and complex oscillation behaviors. The first phenomenon is linked to the prevalence of acetylene formation and its stabilization with respect to the oxidation of the recombination products with two carbon atoms when the

rich mixture temperature is higher than a threshold value. The second is a modulation of the previous mechanism in the sense that, under approximately stoichiometric and lean conditions, the oxidative channel of $C_{(2)}$ species is favored even though it is inhibited by the temperature increase. The recognition of the kinetic routes, which trigger these significant, well-documented phenomena in different regions of air fuel ratio and temperature, is relevant from a practical point of view, because it allows possible behaviors with respect to other parameters which could not be investigated across a wide range because of apparatus limitations, to be inferred. Dilution levels and residence times in particular must be analyzed through their influence on the temperature of combustion products. This is because the higher this temperature is, the less likely there is oscillative or unsteady or unstable behavior. Therefore, the expected temperature increase with the decrease in the residence time or in dilution level is beneficial in suppressing these regimes. This is consistent with the measured and predicted data presented in the previous sections, and it is reasonable to expect it to be realistic across a wider range of operating conditions than those reported in this paper also.

REFERENCES

1. A. Cavaliere, M.de Joannon, *Prog. Energ. Comb. Sci.* 30(4) (2004) 329-366.
2. J.A. Wünnig, J.G. Wünnig, *Prog. Energy Comb. Sci.* (1997) 23-81.
3. M.de Joannon, P. Sabia, A.Tregrossi, A.Cavaliere: *3rd Mediterranean Combustion Symposium*, Marrakech, Morocco, June, (2003) 79.
4. M.Vanpée, *Comb. Sci. Tech.* (1993) 363-374.
5. A. Ciajolo, A. D'Anna, *Combust.Flame.* 112(4) (1998) 617-622.
6. E.Ranzi, M. Dente, A Goldaniga, G. Bozzano, T.Faravelli, *Prog.Energy Combust.Sci.* 27(2001) 99-139.
7. E.Ranzi, A. Sogaro, P. Guffuri, G. Pennati, T. Faravelli, *Comb. Sci. Tech.*96(1994) 279-325.
8. T.Faravelli, P. Gaffuri, E.Ranzi, J.F. Griffiths, *Fuel* 77 (3) (1998) 147-155.
9. Warnatz J., Maas U., Dibble R.W., *Combustion: Physical and Chemical Fundamentals, Modelling and Simulation, Experiments, Pollutant Formation*, Springer, Berlin (1999).
10. Buzzi-Ferraris G., D.Manca, *Computers Chem.Eng.*22 (11)(1998) 1595-1621.
11. CHEMKIN Collection, Release 3.6, Reaction Design, Inc., San Diego, CA (2000).
12. Aurora, CHEMKIN Collection, Release 3.6, Reaction Design, Inc., San Diego, CA (2000).
13. de Joannon, M.,Tregrossi A., Cavaliere A.: *Seventh International Conference on Energy for a Clean Environment*, Lisbon, Portugal, July, 435 (2003).
14. C.K. Westbrook, *Proc. Combust. Inst.* 28 (2000) 1563-1577.
15. M de Joannon, A Cavaliere, R Donnarumma, R Ragucci. *Proc. Combust. Inst*, 29 (2003).
16. R.Weber, S.Orsino, N.Lalleman, A.Verlaan. *Proc. Combust. Inst.* 28 (2000) 1315-1321.
17. M. de Joannon, A. Saponaro, A. Cavaliere, *Proc. Combust. Inst.* 28 (2000) 1639-1646.